Li(Zn,Mn)As as a new generation ferromagnet based on a I–II–V semiconductor

Z. Deng[1], C.Q. Jin[1], Q.Q. Liu[1], X.C. Wang[1], J.L. Zhu[1], S.M. Feng[1], L.C. Chen[1], R.C. Yu[1], C. Arguello[2], T. Goko[2], Fanlong Ning[2,3], Jinsong Zhang[4], Yayu Wang[4], A.A. Aczel[5], T. Munsie[5], T.J. Williams[5], G.M. Luke[5], T. Kakeshita[6], S. Uchida[6], W. Higemoto[7], T.U. Ito[7], Bo Gu[7,8], S. Maekawa[7,8], G.D. Morris[9] & Y.J. Uemura[2]

In a prototypical ferromagnet (Ga,Mn)As based on a III–V semiconductor, substitution of divalent Mn atoms into trivalent Ga sites leads to severely limited chemical solubility and metastable specimens available only as thin films. The doping of hole carriers via (Ga,Mn) substitution also prohibits electron doping. To overcome these difficulties, Masek *et al.* theoretically proposed systems based on a I–II–V semiconductor LiZnAs, where isovalent (Zn,Mn) substitution is decoupled from carrier doping with excess/deficient Li concentrations. Here we show successful synthesis of $Li_{1+y}(Zn_{1-x}Mn_x)As$ in bulk materials. Ferromagnetism with a critical temperature of up to 50 K is observed in nominally Li-excess ($y = 0.05$–0.2) compounds with Mn concentrations of $x = 0.02$–0.15, which have p-type metallic carriers. This is presumably due to excess Li in substitutional Zn sites. Semiconducting LiZnAs, ferromagnetic Li(Zn,Mn)As, antiferromagnetic LiMnAs, and superconducting LiFeAs systems share square lattice As layers, which may enable development of novel junction devices in the future.

[1] Beijing National Laboratory for Condensed Matter Physics, and Institute of Physics, Chinese Academy of Sciences, Beijing 100190, China. [2] Department of Physics, Columbia University, New York, New York 10027, USA. [3] Department of Physics, Zhejiang University, Hangzhou 310027, China. [4] Department of Physics, Tsinghua University, Beijing 100084, China. [5] Department of Physics and Astronomy, McMaster University, Hamilton, Ontario, L8S 4M1 Canada. [6] Department of Physics, University of Tokyo, 7-3-1 Hongo, Bunkyo-Ku, Tokyo 113-8656, Japan. [7] Advanced Science Research Center, Japan Atomic Energy Agency, Tokai 319-1195, Japan. [8] CREST, Japan Science and Technology Agency, Sanbancho, Tokyo 102-0075, Japan. [9] TRIUMF, 4004 Wesbrook Mall, Vancouver, British Columbia, V6T 2A3 Canada. Correspondence and requests for materials should be addressed to C.Q.J. (email: jin@iphy.ac.cn) or to Y.J.U. (email: tomo@lorentz.phys.columbia.edu).

Ferromagnetic systems obtained by doping transition metals into semiconductors[1] have generated extensive studies since early 1990s[2] because of their potential use for spin-sensitive electronics (spintronics) devices[3]. In proto-typical systems based on III–V semiconductors, such as (Ga,Mn)As and (In,Mn)As, substitution of divalent Mn atoms into trivalent Ga or In sites leads to severely limited chemical solubility. Because of this, the specimens are chemically metastable, available only as thin films[1], and their material quality exhibits high sensitivity on preparation methods and heat treatments[4]. This substitution dopes hole carriers together with magnetic atoms, which prohibits electron doping to obtain n-type systems necessary for formation of spintronics p–n junction devices. To overcome these difficulties, Masek et al.[5] theoretically proposed systems based on a I–II–V semiconductor LiZnAs, wherein magnetism due to isovalent (Zn,Mn) substitution may be decoupled with carrier doping with excess/deficient Li concentrations.

LiZnAs is a direct-gap semiconductor that has a cubic crystal structure (Fig. 1a)[6,7] and a band gap (1.61 eV) similar to that of GaAs (1.52 eV)[8]. Monovalent Li and divalent Zn together substitute the role of trivalent Ga (ref. 9). The local density approximation calculation of Masek et al.[5] obtained the band structure very close to that of GaAs. LiMnAs is an antiferromagnet with T_N exceeding 393 K (refs 10,11) that has a tetragonal crystal structure (Fig. 1b). Via (Zn,Mn) substitution and carrier doping with excess/deficient Li concentrations, $Li_{1+y}(Zn_{1-x}Mn_x)As$ with a small x is expected to become ferromagnetic analogous to (Ga,Mn)As (ref. 5). Owing to isovalent (Zn,Mn) substitutions, $Li_{1+y}(Zn_{1-x}Mn_x)As$ may be obtained as chemically stable bulk material for a wide range of x.

Here we report the synthesis of bulk specimens of a new ferromagnet $Li_{1+y}(Zn_{1-x}Mn_x)As$ based on a I–II–V semiconductor, together with characterization of the structural, transport and magnetic properties. Initial values of the ferromagnetic transition temperature T_C reach up to 50 K, and the Li excess specimens exhibit p-type carriers, which may be due to excess Li atoms occupying substitutional Zn sites. Future efforts in optimizing growth conditions and heat treatments, as well as the replacement of alkali metal and pnictogen atoms, may allow the development of systems with higher T_C and synthesize long-awaited n-type electron doped compounds that exhibit spontaneous magnetic order.

Results

Synthesis and structure. Polycrystalline specimens of $Li_{1+y}(Zn_{1-x}Mn_x)$ As were prepared by solid-state reaction with high-purity elements at the Institute of Physics (IOP) in Beijing. The main difficulty was the high chemical activity and volatility of lithium. Initially, excess lithium was used, but it was difficult to account for the exact amount. A sealed metal tube solved this problem. Starting materials with amounts proportional to the nominal element concentrations were loaded into a Ta tube with Ar under 1 atm pressure. Then, the sealed Ta tube was sealed into an evacuated quartz tube. The samples were heated to 700 °C and held for several hours before the temperature was decreased slowly. The powder samples were characterized by X-ray diffraction and dc magnetization at IOP, and sintered pellet samples were examined by electrical resistivity and Hall effect at IOP and Tsinghua and muon spin relaxation (μSR) measurements at TRIUMF, in Vancouver, Canada.

The X-ray measurements showed that $Li_{1+y}(Zn_{1-x}Mn_x)As$ has a crystal structure with the space group F-43 m (Fig. 1a–d). This structure can be viewed as zinc-blend GaAs, in which Ga is replaced by Li and Zn, with Li atoms located at the As tetrahedral interstitial sites. The lattice parameters for $Li_{1+y}(Zn_{1-x}Mn_x)As$ are shown in Figure 1e: $a = 5.940(1)$ Å for LiZnAs is consistent with the reported value[7], and the monotonic behaviour with increasing x suggests successful (Zn,Mn) solid solution. The equilibrium solubility of Mn atoms in III–V compounds is less than 1%, and specimens of (Ga,Mn)As are available only in the form of chemically metastable
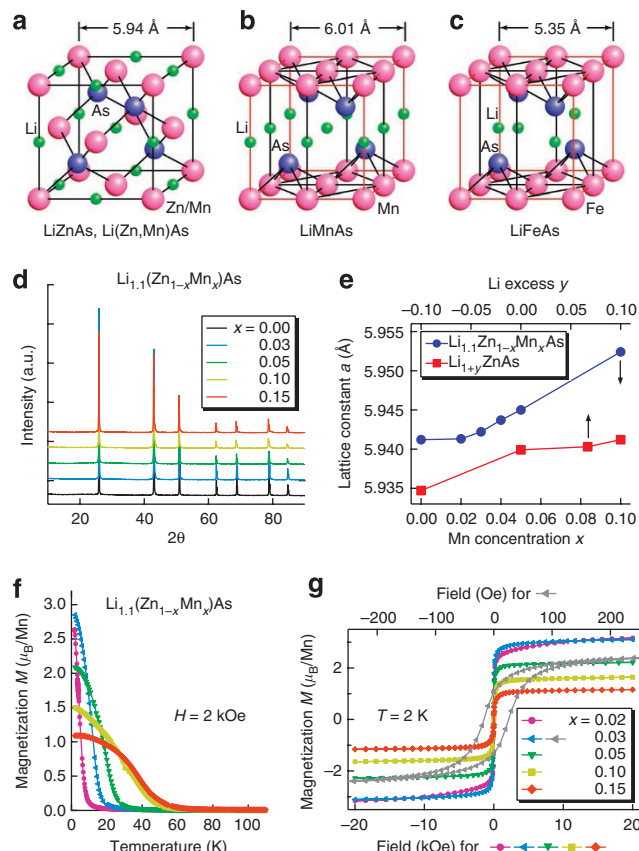
Figure 1 | Crystal structures of Li(Zn,Mn)As and X-ray and magnetization results. (**a–c**): crystal structures of (**a**) cubic LiZnAs (direct-gap semiconductor) and Li(Zn,Mn)As (ferromagnetic metal, as demonstrated in the present work), (**b**) tetragonal LiMnAs (antiferromagnet with T_N>393K), and (**c**) tetragonal LiFeAs (non-magnetic superconductor with T_c~20K). All these structures include square-lattice As layers with the matching of the lattice constant within ~10%. Primitive cells for the tetragonal crystals of (**b**) and (**c**) are shown by the black lines. (**d,e**): X-ray scattering results of (**d**) intensity profile of $Li_{1.1}(Zn,Mn)As$ with various Mn concentrations x, and (**e**) lattice constant of $Li_{1.1}(Zn_{1-x}Mn_x)$ As for various x (blue symbols, bottom horizontal axis), and $Li_{1+y}ZnAs$ (red symbols, top horizontal axis) for various Li deficiency/excess y. (**f,g**): Magnetization $M(H,T)$ results of $Li_{1.1}(Zn_{1-x}Mn_x)As$ with $x = 0.0$–0.15 showing (**f**) the T dependence of M in $H = 2$ kOe (no difference in FC and ZFC procedures) and (**g**) M at $T = 2$ K in various values of external field H. The grey symbols show a hysteresis loop in $x = 0.03$ system plotted for small field regions (top horizontal axis), which demonstrate a very small coercive field of 30–100 Oe.

thin films made by molecular beam epitaxy[1]. In contrast, chemically stable bulk crystals with the cubic structure of LiZnAs can be obtained for Mn concentrations x up to at least 0.15 and Li excess content y ranging $-0.1 \leq y \leq 0.2$. For systems with $0 \leq x \leq 0.15$, excess Li with $0 \leq y$ does not alter the lattice constants, as demonstrated in Figure 1e with the results of $x = 0$, which will be discussed later.

The dc-magnetization M was measured for specimens with nominal Li concentrations 0.9, 0.95, 1.0, 1.05, 1.1 and 1.2 (that is, $-0.1 \leq y \leq 0.2$) and Mn concentration $x = 0$, 0.02, 0.03, 0.05, 0.1 and 0.15. Ferromagnetism was found only in compounds with excess Li ($y \geq 0.05$). Figure 1f shows the temperature dependence of M at 2 kG (no difference between field cooling (FC) and zero-field cooling (ZFC) procedures), whereas Figure 1g shows the field dependences of M at $T = 2$ K, for Li 1.1 systems with various x values. Clear signatures of ferromagnetic order are seen in these figures.

Table 1 | Ferromagnetic transition temperature and ordered moment size.

| Li concentration	1.05		1.1		1.2	
	T_c (K)	M (T=2 K)	T_c (K)	M (T=2 K)	T_c (K)	M (T=2 K)
Mn concentration						
0.03			17	2.9		
0.05			29	2.1	14	1.8
0.1	22	0.6	49	1.5	22	1.4
0.15	38	0.5	50	1.1	23	0.7

M (Bohr magneton per Mn).
The values of T_c and the average ordered moment size M per Mn of $Li_{1+y}(Zn_{1-x}Mn_x)As$ at $T=2K$ and $H=2kOe$ derived from magnetization measurements for several combinations of Li and Mn concentrations.

In Table 1, we list the values of Curie temperature T_c and the spontaneous magnetization $M(T=2K; H=2kG)$ for several combinations of Li and Mn concentrations. The T_c values show a saturation at ~50 K for $x=0.1$–0.15, whereas the ordered moment values per Mn atom show a maximum for low Mn concentrations and decreases monotonically with increasing x. This is presumably due (partly) to an effect of the antiferromagnetic coupling for Mn pairs in the nearest neighbour Zn sites. The lack of history dependence in M and a very thin hysteresis loop in Figure 1g both indicate a very small coercive field (30–100 Oe), which is promising for spin manipulation. In systems with $x \leq 0.1$, the magnetic susceptibility χ at high temperatures above T_c exhibits a simple history-independent Curie–Weiss behaviour with the effective paramagnetic moment values of 5.0–6.0 Bohr magnetons per Mn, as expected for fully magnetic individual Mn^{2+} moments.

Transport. Results of transport studies are shown in Figure 2a–d. Semiconducting behaviour of resistivity of undoped LiZnAs (Fig. 2a) changes to T-independent behaviour for Li deficient systems, wheras much smaller resistivity and definite metallic behaviour were found for Li excess samples with $y \geq 0.05$. Figure 2b shows the resistivity curves of the Li1.1 systems with $x=0$, 0.02, 0.03, 0.05 and 0.10. The resistivity increases monotonically with increasing Mn concentration, suggesting that Mn acts as a scattering centre. The onset of magnetic order reduces this scattering rate, as can be seen in the negative magnetoresistance of Li1.1Mn0.1 system in Figure 2c below T_c.

Because an excess Li (positive y) at an interstitial site is expected to serve as an electron donor, we initially expected n-type carriers for systems with $y \geq 0.05$. However, the Hall effect measurements clearly showed p-type carriers for Li excess systems with all the Mn concentrations ranging from $x=0.0$–0.15. Figure 2d shows representative Hall results for the Li1.1 Mn0.05 system, which exhibits anomalous Hall effect at $H=0$ below T_c and p-type carrier concentration $n \sim 10^{20}$ cm^{-3}. The p-type carrier for excess Li can be expected when the excess Li occupies substitutional Zn sites, and the substituted Zn atoms either escape from the system or remain neutral without ionization. This possibility is supported by flattening of the lattice constant with increasing y in Figure 1e and chemical analyses of the end products that indicate that Zn concentrations are lower than the starting nominal concentrations by about 5–10% for Li excess systems with $y \sim 0.05$–0.1.

Magnetic characterization. Earlier μSR studies of (Ga,Mn)As (ref. 12) demonstrated that ferromagnetism develops in the full volume fraction with sharp transitions for films made by proper heat treatments. To examine volume fraction and the ordered moment size, μSR measurements were performed on $Li_{1.1}(Zn_{0.95}Mn_{0.05})As$ at TRIUMF in Vancouver, Canada. The time spectra observed in zero field (Fig. 3a) clearly exhibit an increase of the relaxation rate below $T \sim 25$ K (Fig. 3b), and measurements in longitudinal fields confirmed that this is due to static magnetic order. The volume fraction
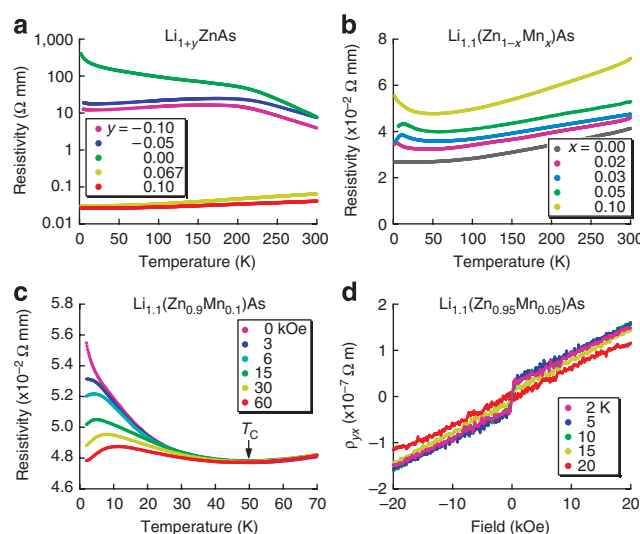

Figure 2 | Results of transport measurements. Transport results of sintered polycrystalline specimens of $Li_{1+y}(Zn_{1-x}Mn_x)As$: (**a**) resistivity of $Li_{1+y}ZnAs$, showing metallic behaviour of Li deficient ($y<0$) and Li excess ($y>0$) compounds. (**b**) resistivity of $Li_{1.1}(Zn_{1-x}Mn_x)As$, showing the effect of increasing charge scattering with increasing Mn concentration x. (**c**) resistivity of $Li_{1.1}(Zn_{0.9}Mn_{0.1})As$ in various external field H, which exhibits negative magnetoresistance below $T_c \sim 50$ K. (**d**) Hall resistivity of $Li_{1.1}(Zn_{0.95}Mn_{0.05})As$ at $T=2$ K, which exhibits p-type carriers with concentrations of $n \sim 10^{20}$ cm^{-3} together with the anomalous Hall effect due to spontaneous magnetization at $H=0$.

of regions with static magnetism (Fig. 3c) indicates a sharp transition at $T_c \sim 25$–30 K, and magnetic order with the full volume fraction achieved below $T \sim 10$ K. Although the transition is very sharp, some coexistence of paramagnetic and ordered volumes can be seen between $T=15$–25 K. Future studies on fabrication methods and heat treatments might help improve spatial homogeneity of the transition. Figure 3d compares the present result on $Li_{1.1}(Zn_{0.95}Mn_{0.05})As$ with those of (Ga,Mn)As with various different Mn concentrations[12] in a plot of the low-temperature relaxation rate versus T_c. A good agreement of the ratio of these two parameters suggests that ferromagnetism of these two systems are very similar in terms of the ordered moment size and concentration (represented by the relaxation rate) and the magnitude of ferromagnetic exchange interaction (which determines T_c). See Methods for details of the μSR data analyses.

Discussion

Availability of bulk crystal specimens is a major advantage of Li(Zn,Mn)As over existing ferromagnets based on III–V semiconductors. This already enabled us to start NMR measurements and obtain promising preliminary results, and plan neutron scattering
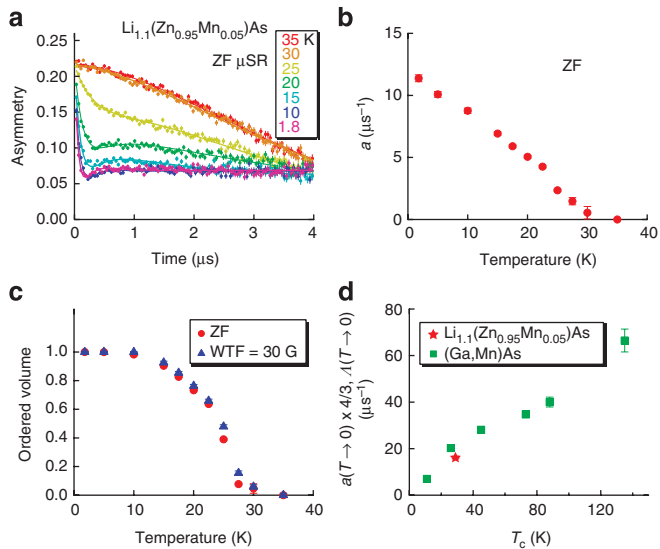
Figure 3 | Results of muon spin relaxation measurements. Results of μSR measurements in sintered polycrystalline specimens of $Li_{1.1}(Zn_{0.95}Mn_{0.05})As$: (**a**) time spectra in zero field that exhibit onset of extra relaxation below T~30 K. The solid lines represent fits to the relaxation function for dilute spin systems in zero field for the static case (often used for dilute-alloy spin glasses[13]), which exhibits a fast relaxation, plus a non-relaxing paramagnetic component (Methods); (**b**) the relaxation rate a of the signal that exhibits fast relaxation; (**c**) the volume fraction of the magnetically ordered region, derived from the amplitude of the fast relaxing signal; (**d**) comparison between the present results (red symbol) and those from (Ga,Mn)As[12] in a plot of the relaxation rate (which is proportional to the individual ordered moment size multiplied by the moment concentration) versus T_c (which is a measure of the effective average ferromagnetic interaction). A factor 4/3 is multiplied to the parameter a to adjust the difference from the simple exponential decay rate Λ adopted in ref. 12. The good agreement implies that the plotted systems have common mechanisms for their ferromagnetism.
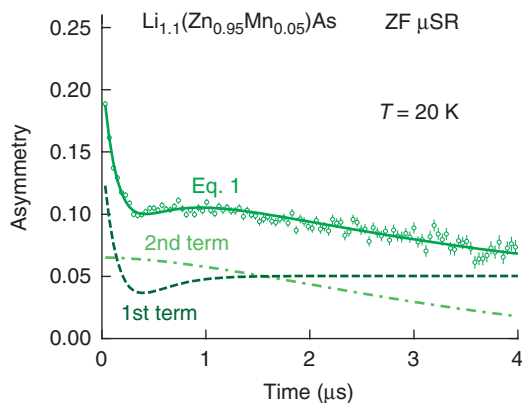
Figure 4 | μSR time spectra in zero field. ZF μSR time spectra in $Li_{1.1}(Zn_{0.95}Mn_{0.05})As$ at $T = 20$ K (open circles). The solid line represents the best fit to equation (1). The black and green broken lines show the first and the second terms, respectively, of this fitting function.

studies to study spin dynamics. As demonstrated in Figure 1a–c, square lattice As layers are commonly included in cubic crystals of semiconducting LiZnAs and ferromagnetic $Li_{1+y}(Zn_{1-x}Mn_x)As$ and tetragonal crystals of antiferromagnetic LiMnAs and superconducting LiFeAs (refs 14–16). The difference of the diagonal As–As distances is within about 10%, and even better lattice matching may be
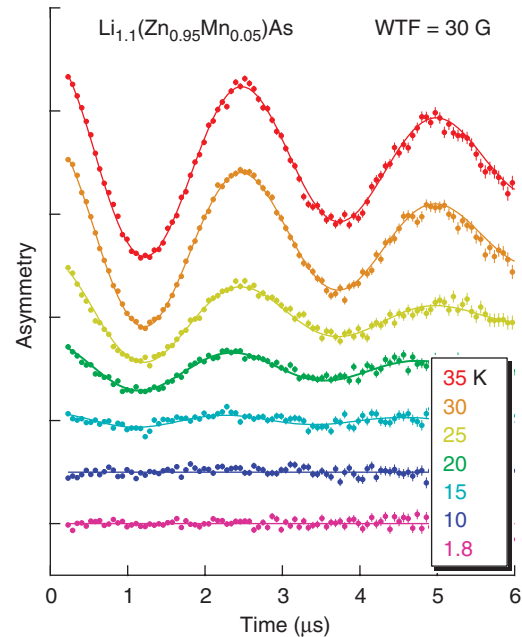
Figure 5 | μSR time spectra in the WTF. μSR time spectra in the WTF of 30 Oe in $Li_{1.1}(Zn_{0.95}Mn_{0.05})As$. The oscillation amplitude corresponds to the paramagnetic volume faction.

expected by replacing Li with other alkali metal elements such as Na and/or replacing As with other pnictogen elements such as P and Sb. This feature could open possibilities of making junctions between various combinations of these systems through the As layers in efforts to develop spintronics devices showing novel functionalities. Thus, we hope that the present demonstration of ferromagnetism in Li(Zn,Mn)As could lead to a new generation of research on magnetic semiconductors and relevant devices.

Methods
Analysis of muon spin relaxation spectra. For the analysis of the zero-field (ZF) μSR time spectra in polycrystalline sample of $Li_{1.1}(Zn_{0.95}Mn_{0.05})As$, we employed the two component function

$$A_{mag}\, G_z^L(t) + A_{para} \exp(-(\lambda t)^\beta). \qquad (1)$$

G_z^L is the relaxation function for a static magnetic field with Lorentzian distribution:

$$f(H_i) = \frac{\gamma_\mu}{\pi} \frac{a}{a^2 + \gamma_\mu^2 H_i^2} (i = x, y, z), \qquad (2)$$

where $\gamma_\mu = 2\pi \times 1.3554 \times 10^4\, s^{-1}\, G^{-1}$ is the gyromagnetic ratio of the muon spin, and a/γ_μ represents a field amplitude for the half-width at half-maximum. The Lorentzian field distribution is expected for dilute Mn moments randomly substituting Zn sites. G_z^L was given by Kubo[17] as:

$$G_z^L(T) = \frac{1}{3} + \frac{2}{3}(1 - at) \exp(-at), \qquad (3)$$

and observed in dilute-alloy spin glasses.[13] We assumed that β is a temperature-independent parameter. The first and second terms of equation (1) represent the magnetically ordered and paramagnetic volumes, respectively. The ZF spectra above 30 K can be fitted to the second term of equation (1) without the first term. The ZF spectra below 10 K can be fitted to the first term alone. As shown in Figure 4, however, both terms are needed to fit spectra in the temperature region between 15 and 25 K, suggesting coexistence of the paramagnetic and magnetically ordered volumes.

The series expansion for equation (3) in terms of at is

$$G_z^L(t) = 1 - \frac{4}{3}at + a^2 t^2 + \dots. \qquad (4)$$

The Maclaurin series for an exponential decay function $G_z(t) = \exp(-\Lambda t)$,

which was employed for the analysis of ZF-μSR spectra in (Ga,Mn)As,[12] is

$$G_z(t) = 1 - \Lambda t + \frac{1}{2}\Lambda^2 t^2 + ... \qquad (5)$$

By comparing the first-order terms of equations (4) and (5), we notice that Λ corresponds to $\frac{4}{3}a$.

Figure 5 shows μSR spectra in a weak transverse field (WTF) of 30 Oe. The WTF μSR measurements provide direct information of the magnetic volume fraction[18]. If the internal magnetic field is much larger than the applied field, the oscillation amplitude can be an indicator of the paramagnetic volume. The good agreement of the ordered fraction derived from the measurements in ZF and those in WTF, shown in Figure 3c, supports the validity of our analysis of ZF-μSR spectra, using the two-component function.

References

1. Ohno, H. Making nonmagnetic semiconductors ferromagnetic. *Science* **281**, 951–956 (1998).
2. Dietl, T. A ten-year perspective on dilute magnetic semiconductors and oxides. *Nature Mater.* **9**, 965–974 (2010).
3. Zutic, I., Fabian, J. & Das Sarma, S. Spintronics: fundamentals and applications. *Rev. Mod. Phys.* **76**, 323–410 (2004).
4. Potashnik, S. J., Ku, K. C., Chun, S. H., Berry, J. J., Samarth, N. & Schiffer, P. Effects of annealing time on defect-controlled ferromagnetism in Ga$_{1-x}$Mn$_x$As. *Appl. Phys. Lett.* **79**, 1495–1497 (2001).
5. Masek, J. *et al.* Dilute moment n-type ferromagnetic semiconductor Li(Zn,Mn)As. *Phys. Rev. Lett.* **98**, 067202 (2007).
6. Bacewicz, R. & Ciszek, T. F. Preparation and characterization of some A^{I}B^{II}C^V type semiconductors. *Appl. Phys. Lett.* **52**, 1150–1151 (1988).
7. Kuriyama, K. & Nakamura, F. Electrical transport properties and crystal structure of LiZnAs. *Phys. Rev. B* **36**, 4439–4441 (1987).
8. Kuriyama, K., Kato, T. & Kawada, K. Optical band gap of the filled tetrahedral semiconductor LiZnAs. *Phys. Rev. B* **49**, 11452–11455 (1994).
9. Wei, S. H. & Zunger, A. Electronic structure and phase stability of LiZnAs: A half ionic and half covalent tetrahedral semiconductor. *Phys. Rev. Lett.* **55**, 528–531 (1986).
10. Bronger, W., Mueller, P., Hoeppner, R. & Schuster, H. U. The magnetic properties of NaMnP, NaMnAs, NaMnSb, NaMnBi, LiMnAs and KMnAs, characterized by neutron-diffraction experiments. *Z. Anorg. Allg. Chem.* **539**, 175–182 (1986).
11. Jungwirth, T. *et al.* Demonstration of molecular beam epitaxy and a semiconducting band structure for I-Mn-V compounds. *Phys. Rev. B 83*, 035321 (2011).
12. Dunsiger, S. R. *et al.* Spatially homogeneous ferromagnetism of (Ga,Mn)As. *Nature Mater.* **9**, 299–303 (2010).
13. Uemura, Y. J., Yamazaki, T., Harshman, D. R., Senba, M. & Ansaldo, E. J. Muon-spin relaxation in AuFe and CuMn spin glasses. *Phys. Rev. B* **31**, 546–563 (1985).
14. Wang, X. C. *et al.* The superconductivity at 18K in LiFeAs system. *Solid State Commun.* **148**, 538–540 (2008).
15. Pitcher, M. J., Parker, D. R., Adamson, P., Herkelrath, S. J. C., Boothroyd, A. T. & Clarke, S. J. Structure and superconductivity of LiFeAs. *Chem. Commun.* **45**, 5918–5920 (2008).
16. Chu, C. W. *et al.* The synthesis and characterization of LiFeAs and NaFeAs. *Physica C* **469**, 326–331 (2009).
17. Kubo, R. A stochastic theory of spin relaxation. *Hyperfine Interact.* **8**, 731–738 (1981).
18. Uemura, Y. J. *et al.* Phase separation and suppression of critical dynamics at quantum phase transitions of MnSi and (Sr$_{1-x}$Ca$_x$)RuO$_3$. *Nat. Phys.* **3**, 29–35 (2007).

Acknowledgements

Author contributions

Y.J.U. proposed the project. Y.J.U. and C.Q.J. planned and arranged the collaboration. C.Q.J., Z.D., Q.Q.L., X.C.W., J.L.Z., S.M.F., L.C.C. and R.C.Y. carried out the synthesis and magnetization measurements. C.Q.J., Z.D., Q.Q.L., X.C.W., J.L.Z., S.M.F., L.C.C., R.C.Y., J.Z., Y.W., T.K. and S.U. carried out the transport measurements. C.A., T.G., F.N., A.A.A., T.M., T.J.W., G.M.L., G.D.M., W.H., T.U.I. and Y.J.U. carried out μSR measurements. B.G. and S.M carried out theoretical discussions. T.G. and Y.J.U. wrote the methods. Z.D., C.Q.J. and Y.J.U. prepared the draft manuscript.

Additional information

Competing financial interests: The authors declare no competing financial interests.

Reprints and permission information is available online at http://npg.nature.com/reprintsandpermissions/

How to cite this article: Deng, Z. *et al.* Li(Zn,Mn)As as a new generation ferromagnet based on a I-II-V semiconductor. *Nat. Commun.* 2:422 doi: 10.1038/ncomms1425 (2011).